The Structure of Liquid Water by Neutron Scattering. II. Temperature Dependence of the Liquid Structure

Norio Ohtomo,† Kazuo Tokiwano,† and Kiyoshi Arakawa*

Research Institute of Applied Electricity, Hokkaido University, Sapporo 060

† *Faculty of Engineering, Hokkaido University, Sapporo 060*

(Received March 1, 1982)

The structure factors for heavy water at 25, 50, 70, and 95 °C were determined in the range of Q, 1.4—20 Å^{-1}, by means of the time-of-flight (TOF) neutron diffraction method using the electron linear accelerator (LINAC). An analysis of the neutron diffraction data was made by applying a new general theoretical procedure of analysis for the fluid system composed of molecular clusters with various sizes. Structure factors were calculated according to the general procedure for the pentamer-monomer mixture model as a mixture of regular tetrahedral pentamers and non-bonded monomers with a due assignment of pentamer fraction at each temperature. Excellent agreement was obtained between the calculated and observed structure factors at temperatures in 25—95 °C. Combined with the preceding result (N. Ohtomo, K. Tokiwano, and K. Arakawa, *Bull. Chem. Soc. Jpn.*, **54**, 1802 (1981)), it was concluded that the pentamer-monomer mixture model is the best one for water from room temperature to near the boiling point.

In the preceding paper[1]# we reported an analysis of the liquid structure of water by combining neutron and X-ray diffraction data, and showed that liquid water at room temperature has a basic structure as an aggregate of regular tetrahedral pentamers. The analysis was performed concerning the structure of water only at a temperature, 15 °C. Then, we attempt here to perform structure analysis of liquid water at more elevated temperatures. For this purpose, we have carried out a neutron diffraction measurement on water at 25—95 °C, and further, have made an analysis of the data by applying a newly devised theoretical procedure of analysis for the fluid system composed of molecular clusters with various sizes.

Neutron Diffraction Data

Measurement. Neutron scattering intensities were measured for liquid water at 25, 50, 70, and 95 °C by means of the LINAC-TOF neutron diffraction method. Basic architecture of the diffractometer and experimental procedures were reported elsewhere.[2] In the present study measurements were made simultaneously at two scattering angles ($2\theta=40°$ and 65°). Neutrons scattered towards two directions were detected in a bifurcated array of two counters (Fig. 1). The angular divergence of the Soller slit as a collimator, which governs primarily the resolving power, was 30′ and 38′ for the slit used at lower and higher scattering angles, respectively.

A sample of 99.9% deuterium oxide contained in a thin-walled cylindrical quartz vessel (100 mm long, 10 mm internal diameter, and 0.1 mm wall thickness) was placed within a thin aluminum cylindrical reflector of an elliptical contour (Fig. 1). A Digital Thermometer (FLUKE Model 2190A) and a rod heater were used, and the vertical axis of the heating rod and the cylindrical sample container are placed exactly at the two focussing points of the elliptic contour. Temperature measurement was made by thermocouples inserted into the top and bottom of the sample. The temperature was controlled within the fluctuation of 1 °C through all the measurements in the present experiment (Fig. 2).

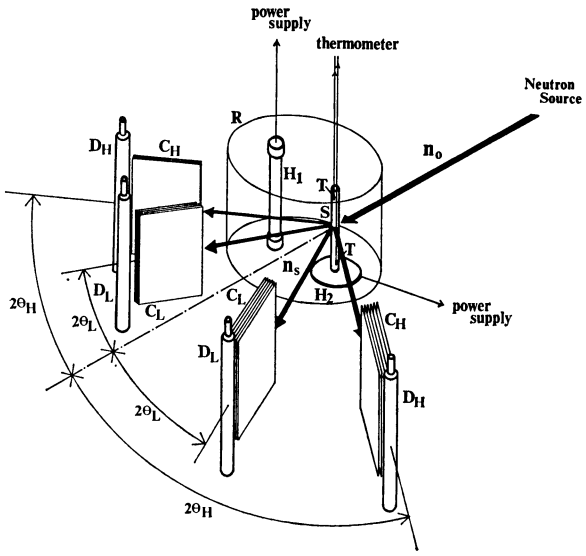

Fig. 1. A perspective view of the diffractometer. n_0: Incident neutron beam, n_s: scattered neutron beam, S: sample, H_1: heater rod, H_2: auxiliary heater, R: reflector, T: thermocouple, C: Soller collimator, D: detector, 2θ: scattering angle. Suffixs H and L denote higher and lower scattering angles, respectively.

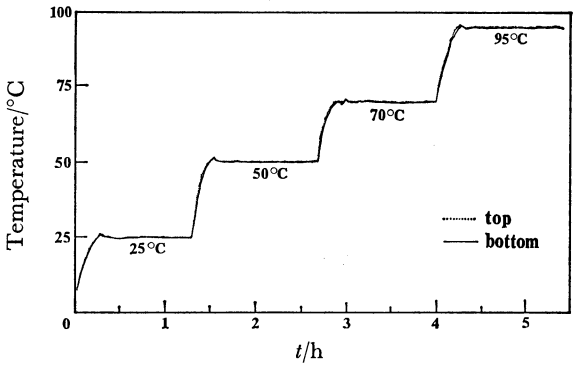

Fig. 2. Temperature of D_2O sample through all the measurements.

Correction Procedures and Structure Factors. For obtaining the structure factors $S_m(Q)$ from the measured raw data, several corrections (multiple scattering, ab-

We cite Ref. 1 as paper I in the following.

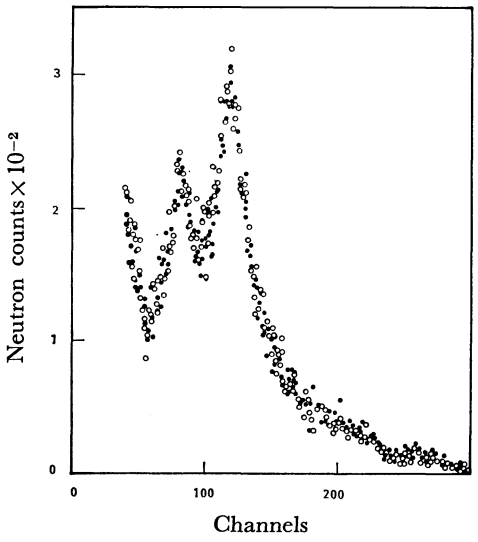

Fig. 3. Temperature variation of background counting including the scattering from the container ($2\theta=65°$).
○: 25 °C, ●: 95 °C.

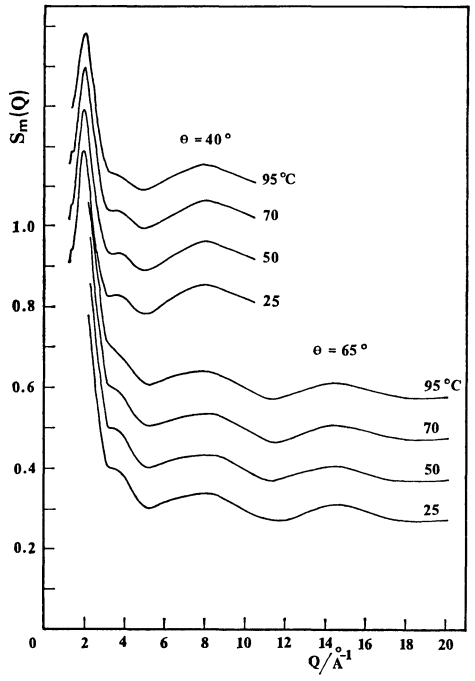

Fig. 4. Partially-corrected neutron structure factors $S_m(Q)$ (corrected with respect to background counting, multiple scattering, and absorption).

sorption, background counting, inelastic scattering, and incoherent scattering) and absolute normalization of data were carried out according to similar procedures as made in the preceding studies.[2-4] In applying these correction procedures to the present raw data, however, a due consideration on the influence of temperature variations must have been taken into account. In order to examine the temperature variation of background counting including the scattering from the container, we measured the intensity of neutrons scattered from the empty container at two temperatures (25 and 95 °C). It was found that differences between the

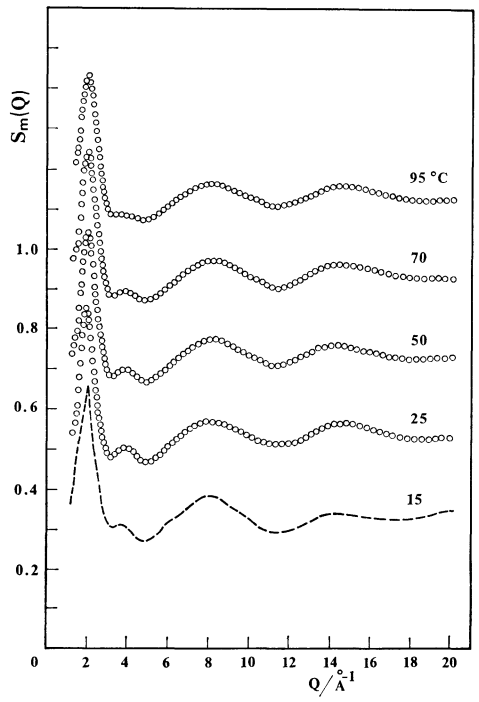

Fig. 5. Observed neutron structure factors $S_m(Q)$ for heavy water at 25, 50, 70, and 95 °C, together with the previous data at 15 °C.

two temperatures were negligibly small (Fig. 3). This is attributed to the thin wall-width of the container. Then, for the background counting, we could safely use the value at 25 °C through all the temperatures. With respect to multiple scattering and absorption, the temperature-dependent variation was assumed to be negligible for the temperature range in the present study. The partially-corrected $S_m(Q)$ curves after corrected with respect to background counting, multiple scattering, and absorption are shown in Fig. 4.

With respect to inelastic scattering which is important for D_2O, the following feature is clearly seen in Fig. 4. All the $S_m(Q)$ data at the same scattering angle at different temperatures are in full agreement with each other except the first peak and the hump at 4 Å^{-1}. This indicates that the inelastic correction is insensitive to temperature variation within the range of the present experiment. The $S_m(Q)$ data at $2\theta=65°$ in Fig. 4 exhibit a larger effect due to inelastic scattering than the data at $2\theta=40°$. This is explained theoretically as follows: the greater descending trend in the $S_m(Q)$ curve with increasing Q at larger scattering angle is typical of the Placzek corrections[5] and is almost entirely due to the self-scattering by the deuterons.[5,6] It can be said that the inelastic correction contributes a temperature-independent monotonic variation as a function of Q. Thus, the Placzek and Wick correction methods used in the previous studies at room temperature[2-4] were safely applied to the present data in lower and higher Q region, respectively, at 25—95 °C.

Absolute normalization of data was carried out with the use of scattering data from a vanadium standard. Calibration of absolute values for high Q data was performed according to the limiting procedure that

$S_m(Q)\to\Sigma b_n^2/(\Sigma b_n)^2$ as $Q\to\infty$, where incoherent scattering is duely considered. Calibration for low Q data was done by overlapping the $S_m(Q)$ curves in the Q range of 3—5 Å^{-1}. Combining the two corrected data at each scattering angle, the final $S_m(Q)$ curves for a range of Q=1.4—10.5 Å^{-1} and those for a range of Q=2.5—20 Å^{-1} were obtained from the data sets of $2\theta=40°$ and from those of $2\theta=65°$, respectively. The values are tabulated in Table 1. These data at two angles at the same temperature agree very well in the region of Q=2.5—10.5 Å^{-1} (Table 1). Thus, by combining these data at two angles, we obtain the final $S_m(Q)$ curves at each temperature as shown in Fig. 5, together with the curve at 15 °C obtained previously.[1] A marked feature of the structure factors obtained is a gradual falling of the hump at *ca.* 4 Å^{-1} as the temperature is raised.

Experimental accuracy has been improved at more satisfactory level in this study. The statistical error for values of $S_m(Q)$ is smaller than 0.5% in the range of Q=2—6 Å^{-1}, and the resolving power $\Delta Q/Q$ less than a few % in the whole range of Q.

Theoretical Procedure of Analysis

Theory. In paper I we derived a formula of $S_m(Q)$ for liquid consisting of identical clusters (Eqs. 7—11 in I). For the analysis of the present data, the $S_m(Q)$ formula for liquid composed of molecular clusters of various sizes including monomers is required. In the following, we will state the details of derivation of the formula, which is an extension of the theory reported in I, with the addition of due assumptions.

The coherent neutron structure factor $S_m(Q)$ is given in general by

$$S_m(Q)=N_m^{-1}\Sigma^{-2}\langle\sum_{i,j}\sum_{n_i,n_j} b_{n_i}b_{n_j}\exp(i\vec{Q}\cdot\vec{r}_{n_in_j})\rangle, \tag{1}$$

where i and j label molecules in a liquid and n_i denotes the n-th nucleus in the molecule i. $\vec{r}_{n_in_j}$ is the vector distance between the nuclei n_i and n_j, b_{n_i} the scattering length of nucleus n_i, $\vec{Q}$ the scattering vector, and $\Sigma=\sum_n b_n$. We sum over all the scatterers in the N_m molecules in the system.

We now consider the case of a fluid system consisting of molecular cluster of various sizes including monomers, where the number of clusters composed of ν molecules is N_ν, and its fraction in molecular number x_ν.

$$x_\nu=\frac{\nu N_\nu}{N_m},\quad\text{and}\quad\sum_\nu \nu N_\nu=\sum_\nu x_\nu N_m=N_m,\qquad(\nu=1,2,\cdots).$$

Then, Eq. 1 is written as follows,

$$S_m(Q)=N_m^{-1}\Sigma^{-2}\langle\sum_\nu\sum_{\alpha_\nu}\sum_{l,l'}\sum_{n_l,n_{l'}} b_{n_l}b_{n_{l'}}\exp(i\vec{Q}\cdot\vec{r}_{n_ln_{l'}})\rangle + N_m^{-1}\Sigma^{-2}\langle\sum_{\nu,\mu}\sum_{\substack{\alpha_\nu,\beta_\mu\\(\alpha_\nu\neq\beta\mu)}}\sum_{l,\kappa}\sum_{n_l,n_\kappa} b_{n_l}b_{n_\kappa}\exp(i\vec{Q}\cdot\vec{r}_{n_ln_\kappa})\rangle, \tag{2}$$

α_ν denotes the α-th cluster in the clusters composed of ν molecules, β_μ the β-th one in the ones composed of μ molecules ($\alpha_\nu=1,\cdots,N_\nu$ and $\beta_\mu=1,\cdots,N_\mu$), l and l′ the l-th and l′-th molecule within the cluster α_ν (l, l′: $1,\cdots,\nu$) respectively, and κ the κ-th molecule within the cluster β_μ($\kappa=1,\cdots,\mu$). The first term in Eq. 2 is the contribution of atom pairs within clusters and the second term the one of inter-cluster atom pairs.

Let us use $\vec{r}_{cll'}$ to denote the vector distance from the center of the l-th molecule to that of the l′-th one within the cluster α_ν, and $\vec{r}_{cl\kappa}$ the vector distance from the center of the l-th molecule in the cluster α_ν to the center of the κ-th molecule in the cluster β_μ. Then, $\vec{r}_{n_ln_{l'}}=\vec{r}_{cll'}-\vec{r}_{cn_l}+\vec{r}_{cn_{l'}}$ and $\vec{r}_{n_ln\kappa}=\vec{r}_{cl\kappa}-\vec{r}_{cn_l}+\vec{r}_{cn_\kappa}$, where $\vec{r}_{cn_l}$ is the vector distance from the center of the molecule l to its n_l-th nucleus, and Eq. 2 is rewritten as follows,

$$S_m(Q)=N_m^{-1}\Sigma^{-2}\langle\sum_\nu\sum_{\alpha_\nu}\sum_{l,l'}\exp(i\vec{Q}\cdot\vec{r}_{cll'})\sum_{n_l,n_{l'}} b_{n_l}b_{n_{l'}}\times\exp\{i\vec{Q}\cdot(-\vec{r}_{cn_l}+\vec{r}_{cn_{l'}})\}\rangle + N_m^{-1}\Sigma^{-2}\langle\sum_{\nu,\mu}\sum_{\substack{\alpha_\nu,\beta_\mu\\(\alpha_\nu\neq\beta\mu)}}\sum_{l,\kappa}\exp(i\vec{Q}\cdot\vec{r}_{cl\kappa})\sum_{n_l,n_\kappa} b_{n_l}b_{n_\kappa}\times\exp\{i\vec{Q}\cdot(-\vec{r}_{cn_l}+\vec{r}_{cn_\kappa})\}\rangle. \tag{3}$$

We adopt here the following assumption: all clusters of equal size have an identical structure on the average (assumption I). Then, the first term of Eq. 3 becomes as follows,

the first term in Eq. 3

$$=N_m^{-1}\Sigma^{-2}\sum_\nu N_\nu\langle[\sum_{l,l'}\exp(i\vec{Q}\cdot\vec{r}_{cll'})\sum_{n_l,n_{l'}} b_{n_l}b_{n_{l'}}\times\exp\{i\vec{Q}\cdot(-\vec{r}_{cn_l}+\vec{r}_{cn_{l'}})\}\rangle, \tag{4}$$

and further, with respect to the second term in Eq. 3, we assume that $\vec{r}_{cl\kappa}$, $\vec{r}_{cn_l}$, $\vec{r}_{cn\kappa}$ are all statistically independent. That is, the molecules belonging to different clusters are assumed to be orientationally-uncorrelated (assumption II). Then,

the second term in Eq. 3

$$=N_m^{-1}\Sigma^{-2}\sum_{\nu,\mu}\sum_{\alpha_\nu,\beta_\mu}\langle\sum_{l,\kappa}\exp(i\vec{Q}\cdot\vec{r}_{cl\kappa})\rangle\times\langle\sum_{n_l} b_{n_l}\exp(-i\vec{Q}\cdot\vec{r}_{cn_l})\rangle\langle\sum_{n_\kappa} b_{n_\kappa}\exp(i\vec{Q}\cdot\vec{r}_{cn_\kappa})\rangle - N_m^{-1}\Sigma^{-2}\sum_\nu N_\nu\sum_{l,l'}\langle\exp(i\vec{Q}\cdot\vec{r}_{cll'})\rangle\times\langle\sum_{n_l} b_{n_l}\exp(-i\vec{Q}\cdot\vec{r}_{cn_l})\rangle\langle\sum_{n_{l'}} b_{n_{l'}}\exp(i\vec{Q}\cdot\vec{r}_{cn_{l'}})\rangle. \tag{5}$$

From Eqs. 3—5, the $S_m(Q)$ for the liquid becomes

$$S_m(Q)=\sum_\nu\frac{x_\nu}{\nu}f^\nu(Q) + N_m^{-1}\Sigma^{-2}\sum_{\nu,\mu}\sum_{\alpha_\nu,\beta_\mu}\sum_{l,\kappa}\langle\exp(i\vec{Q}\cdot\vec{r}_{cl\kappa})\rangle\times\langle\sum_{n_l} b_{n_l}\exp(-i\vec{Q}\cdot\vec{r}_{cn_l})\rangle\langle\sum_{n_\kappa} b_{n_\kappa}\exp(i\vec{Q}\cdot\vec{r}_{cn_\kappa})\rangle, \tag{6}$$

where

$$f^{\nu}(Q) = \Sigma^{-2}[\langle \sum_{l,l'} \exp(i\vec{Q}\cdot\vec{r}_{cll'}) \sum_{n_l,n_{l'}} b_{n_l}b_{n_{l'}} \times \exp\{i\vec{Q}\cdot(-\vec{r}_{cn_l}+\vec{r}_{cn_{l'}})\}\rangle - \sum_{l,l'}\langle\exp(i\vec{Q}\cdot\vec{r}_{cll'})\rangle\langle\sum_{n_l} b_{n_l}\exp(-i\vec{Q}\cdot\vec{r}_{cn_l})\rangle \times\langle\sum_{n_{l'}} b_{n_{l'}}\exp(i\vec{Q}\cdot\vec{r}_{cn_{l'}})\rangle]_{\nu}. \quad (7)$$

In order to express the second term in Eq. 6 as a practically applicable form, we take the factor $\langle \sum_{n_l} b_{n_l}\exp(i\vec{Q}\cdot\vec{r}_{cn_l})\rangle$ to be independent of ν and replace it by the averaged value

$$\left\{\sum_{\nu}\frac{x_{\nu}}{\nu}\left[\sum_{l}[\sum_{n_l} b_{n_l}\langle\exp(i\vec{Q}\cdot\vec{r}_{cn_l})\rangle]^2\right]_{\nu}\right\}^{1/2}, \quad \text{(assumption III)}. \quad (8)$$

Thus, we obtain finally the formula for the $S_m(Q)$ in the form

$$S_m(Q) = \sum_{\nu}\frac{x_{\nu}}{\nu}f^{\nu}(Q) + S_c(Q)\cdot\bar{f}_{2U}(Q), \quad (9)$$

$$S_c(Q) = N_m^{-1}\langle\sum_{i,j}\exp(i\vec{Q}\cdot\vec{r}_{cij})\rangle = 1 + N_m^{-1}\langle\sum_{i\neq j}\exp(i\vec{Q}\cdot\vec{r}_{cij})\rangle, \quad (10)$$

$$\bar{f}_{2U}(Q) = \Sigma^{-2}\sum_{\nu}\frac{x_{\nu}}{\nu}\left[\sum_{l}[\sum_{n_l} b_{n_l}\langle\exp(i\vec{Q}\cdot\vec{r}_{cn_l})\rangle]^2\right]_{\nu}. \quad (11)$$

The Eqs. 7—11 are an extension of the formula Eqs. 7—11 in I, which are applicable to the liquid consisting of molecular clusters of various sizes including monomer molecules. For $x_{\mu}=1$ and $x_{\nu(\neq\mu)}=0$, Eq. 9 reproduces Eq. 7 in I.

Further, in order to elucidate the physical meaning of Eqs. 7—11, we rewrite Eq. 9 and obtain, separating the intramolecular contribution from the intermolecular one, in the form

$$S_m(Q) = \sum_{\nu}\frac{x_{\nu}}{\nu}f_1^{\nu}(Q) + \bar{f}_{2U}(Q)[S_c(Q)-1] + \sum_{\nu\geqq 2}\frac{x_{\nu}}{\nu}f_c^{\nu}(Q), \quad (12)$$

$$f_1^{\nu}(Q) = \Sigma^{-2}[\langle\sum_{l}|\sum_{n_l} b_{n_l}\exp(i\vec{Q}\cdot\vec{r}_{cn_l})|^2\rangle]_{\nu}, \quad (13)$$

and

$$f_c^{\nu}(Q) = \Sigma^{-2}[\langle\sum_{l\neq l'}\exp(i\vec{Q}\cdot\vec{r}_{cll'})\sum_{n_l,n_{l'}} b_{n_l}b_{n_{l'}} \times\exp\{i\vec{Q}\cdot(-\vec{r}_{cn_l}+\vec{r}_{cn_{l'}})\rangle - \sum_{l\neq l'}\langle\exp(i\vec{Q}\cdot\vec{r}_{cll'})\rangle\langle\sum_{n_l} b_{n_l}\exp(-i\vec{Q}\cdot\vec{r}_{cn_l})\rangle \times\langle\sum_{n_{l'}} b_{n_{l'}}\exp(i\vec{Q}\cdot\vec{r}_{cn_{l'}})\rangle]_{\nu}, \quad (14)$$

where $f_1^{\nu}(Q)$ is the intramolecular contribution within the cluster composed of ν molecules. The first sum $\sum_{\nu}(x_{\nu}/\nu)f_1^{\nu}(Q)$ $(\equiv f_1(Q))$ is the overall averaged intramolecular contribution in the liquid. The Eqs. 12—14 are compared to Eqs. 176—179 in a text by Hansen and McDonald[7] (originally derived by Gubbins *et al.*[8,9]), though the latters are impractical except for very simple cases because of the difficulties arising from the calculation of higher order spherical harmonics expansions. The third term $\sum_{\nu}(x_{\nu}/\nu)f_c^{\nu}(Q)$ in Eq. 12 corresponds to the sum of the higher order expansion terms in Gubbins *et al.*'s formula.

In the expression of Eq. 9, it can be seen that for $Q\to 0$ $S_m(Q)\to S_c(Q)$ because $f^{\nu}(Q)\to 0$ and $\bar{f}_{2U}(Q)\to 1$. On the other hand, in the expression of Eq. 12, $S_m(Q)\to f_1(Q)$ when $Q\to\infty$ as is directly seen.

Structure Factor $S_m(Q)$ for the Pentamer–Monomer Mixture Model. From Eqs. 7—11, we can give here the formula of $S_m(Q)$ for the pentamer–monomer mixture model[10,11] for the later analysis of neutron diffraction data, where the form of the pentamer is such as shown in Fig. 3 of paper I. In this case, we put $x_1\neq 0$ and $x_5\neq 0$ (others=zero). Eq. 9 becomes

$$S_m(Q) = x_1 f^1(Q) + \frac{x_5}{5}f^5(Q) + \bar{f}_{2U}(Q)S_c(Q), \quad (15)$$

where the factors $f^1(Q)$ and $f^5(Q)$ are expressed by applying Eq. 7 for the case of $\nu=1$ and $\nu=5$, respectively, as

$$f^1(Q) = f_1^1(Q) - f_{2U}^1(Q) = f_1^1(Q) - \Sigma^{-2}[\sum_{n} b_n\langle\exp(i\vec{Q}\cdot\vec{r}_{cn})\rangle]^2_{\nu=1} \quad (16)$$

and

$$\frac{1}{5}f^5(Q) = S_m^p(Q) - f_{2U}^5(Q)[S_{m,p}^{(00)}(Q)+1] = S_m^p(Q) - \Sigma^{-2}\frac{1}{5}\sum_{l}^{5}[\sum_{n_l} b_{n_l}\langle\exp(i\vec{Q}\cdot\vec{r}_{cn_l})\rangle]^2_{\nu=5} \times[S_{m,p}^{(00)}(Q)+1]. \quad (17)$$

The factor $f_1^1(Q)$ is the intramolecular structure factor for monomer molecules and the two factors, $f_{2U}^1(Q)$ and $f_{2U}^5(Q)$, are the molecular form factor for monomers and pentamers, respectively, which are given in relation to the assumption II. $S_m^p(Q)$ is the intra-pentamer structure factor (Eq. 13 in I) and $S_{m,p}^{(00)}(Q)$ the contribution from intra-pentamer O–O pairs only (Eq. 16 in I). For $x_5=1$ and $x_1=0$, Eq. 9 becomes Eq. 12 in I and for $x_1=1$ and $x_5=0$ we obtain a formula for the completely-uncorrelated orientation model proposed by Egelstaff, Page, and Powles.[12,13]

Eq. 12 becomes

$$S_m(Q) = x_1 f_1^1(Q) + \frac{x_5}{5}f_1^5(Q) + \bar{f}_{2U}(Q)[S_c(Q)-1] + \frac{x_5}{5}f_c^5(Q). \quad (18)$$

The first two terms in Eq. 18 are the averaged intramolecular structure factor for the pentamer–monomer mixture and are grouped as $f_1(Q)$ according to the definition described above,

$$x_1 f_1^1(Q) + \frac{x_5}{5}f_1^5(Q) = f_1(Q). \quad (19)$$

$f_1^5(Q)$ $(\equiv 5S_m^{(1)}(Q)$, Eq. 15 in I) in Eq. 18 is the intramolecular contribution within the pentamer and $f_c^5(Q)$ is obtained from Eq. 14 for the case of $\nu=5$ as

$$\frac{x_5}{5}f_c^5(Q) = x_5[S_m^p(Q) - \frac{1}{5}f_1^5(Q) - f_{2U}^5(Q)S_{m,p}^{(00)}(Q)]. \quad (20)$$

Interpretation of Experimental Data

Procedure of Calculation of the $S_m(Q)$ of Pentamer–Monomer Mixture Model. Now, we can determine the liquid structure of water at each temperature by making the calculated $S_m(Q)$ curve fit with the observed curve shown in Fig. 5. In the preceding study (paper I) it has turned out that the liquid structure of water at 15 °C can be regarded as an aggregate of the regular tetrahedral pentamers. This is the case $x_5=1$ and $x_1=0$ in Eqs. 15—17. At more elevated temperatures, a part of the pentamers is supposed to be destroyed. Then, we can use here Eqs. 15—17 for the calculation of the $S_m(Q)$ of the pentamer-monomer mixture model with due assignment of x_5 values as parameter.

In applying Eqs. 15—17, the structure of the pentamer is taken to be identical with that shown in Fig. 3 in I ($r_{OD}=0.98$ Å, $r_{DD}=1.60$ Å, and DOD angle= 109.5°) and the molecular structure of the monomer is that for the vapour ($r_{OD}=0.96$ Å, $r_{DD}=1.52$ Å, and DOD angle=104.5°).[1,2,14] For the molecular-centers structure factor of the liquid, $S_c(Q)$, the observed X-ray intensity data reported by Narten and Levy (25, 50, 75, and 100 °C)[15] were used, together with the data by Hajdu *et al.* (25 and 50 °C)[16] when required for comparison. Some appreciable differences are observed in these X-ray data, especially with respect to the first peak, and a discussion for the X-ray data will be made in the later section.

Figure 5 shows that a monotonous falling of the main peak at 2 Å^{-1} and the neighboring hump at *ca.* 4 Å^{-1} is produced by increasing temperature while the $S_m(Q)$ curves are quite unchanged in the range of $Q\gtrsim 6$ Å^{-1}. This latter fact is explained as: the $S_m(Q)$ in higher Q region is determined primarily by the intramolecular contribution only. The main interest in recent studies of liquid water has been, thus, concentrated upon the behaviors of the $S_m(Q)$ curves in the region of $Q\lesssim 6$ Å^{-1}.[1,13,17]

Determination of the Best Fit Model by Comparison of $S_m(Q)_{calcd}$ with $S_m(Q)_{obsd}$. We first determined the value of pentamer fraction x_5 by fitting the calculated $S_m(Q)$ curves with the experimental data. The calculated $S_m(Q)$ associated with the variation of x were compared with the observed neutron $S_m(Q)$ data at 25, 50, 70, and 95 °C, respectively, in Fig. 6. For the experimental data at 25 °C, the best fit $S_m(Q)$ curve was obtained in the case of $x_5=0.85$, at 50 °C $x_5=0.75$, at 70 °C $x_5=0.65$, and 95 °C $x_5=0.55$. The agreement of the calculated $S_m(Q)$ curves with the experimental ones is very excellent at all temperatures. Taking account of experimental errors, the deviations of x_5 are found to be ± 0.05 for all cases. The x_5 values determined are shown in Fig. 7 including the result for the data at 15 °C reported in I.

Thus, the variation of the structure of liquid water with temperature is fundamentally explained by the pentamer-monomer mixture model with appropriate pentamer fractions according to Eqs. 15—17. It is concluded that liquid water is regarded as a mixture of regular tetrahedral pentamers and non-hydrogen-bonded monomers at 25—95 °C.

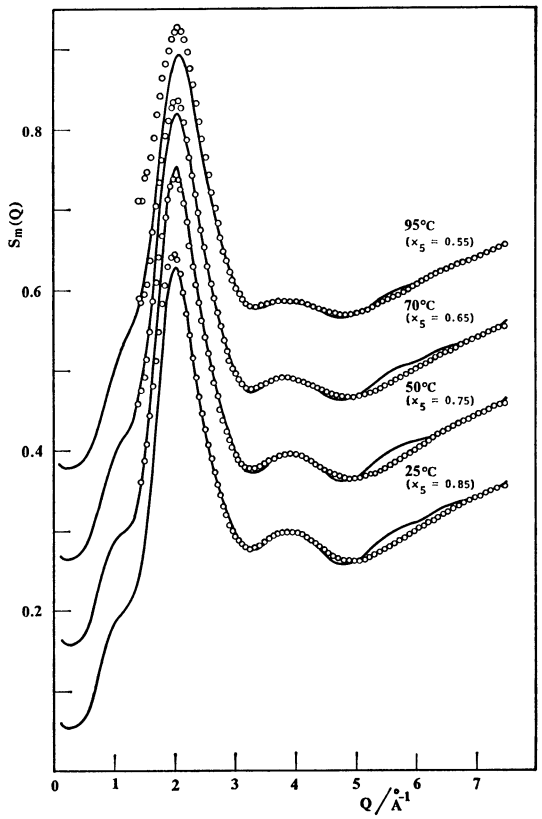

Fig. 6. The comparison between the calculated $S_m(Q)$ for the pentamer-monomer mixture model and the observed neutron structure factors $S_m(Q)$.
○: Observed, ——: calculated.

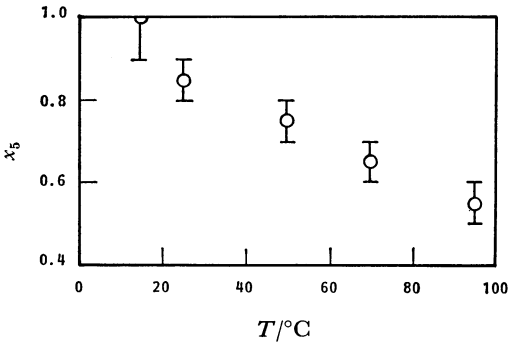

Fig. 7. Pentamer fraction x_5 determined by fitting the $S_m(Q)_{calcd}$ with the $S_m(Q)_{obsd}$ at each temperature. The vertical rod indicates the range of deviations of x_5.

Change of the Principal Peak at 2 Å^{-1} with Temperature. As seen in Table 1, when the temperature is raised, the intensity of the principal peak at *ca.* 2 Å^{-1} is found to decrease gradually, while the position of that to shift slightly to the higher Q-value side. Temperature dependence of the peak intensity and that of its position are shown in Figs. 8(a) and (b), respectively. The trend of the intensity change of the calculated result agrees with that of the experimental data, and the absolute intensity is in agreement with the measured one within the spread of the X-ray data used for $S_c(Q)$. With respect to the shift in the position

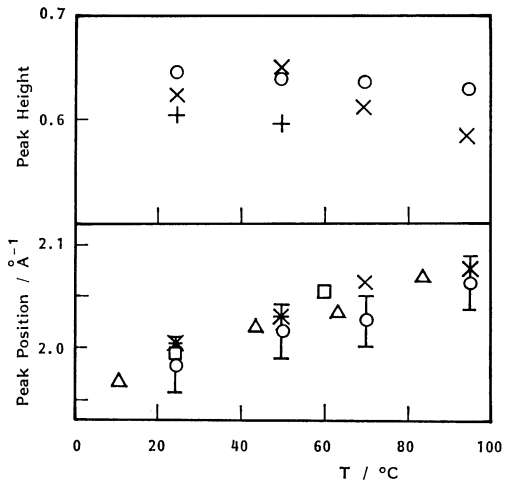

Fig. 8. The change of the intensity and the position of the principal peak at 2 Å^{-1} with the variation of temperature.
○: Observed by the authors, △: observed by Walford and Dore ($\lambda_0=1.13$ Å),[17] □: observed by Walford and Dore ($\lambda_0=0.84$ Å),[17] ×: calculated by the authors with the use of Narten and Levy's X-ray intensity data,[15] +: calculated by the authors with the use of Hajdu *et al.*'s X-ray intensity data.[16]

of the peak, the agreement between the calculated and observed results is very good as a whole within the experimental accuracy.

X-Ray Intensity Data. We used the observed X-ray intensity data mainly provided by Narten and Levy[15] for the calculation of $S_c(Q)$. The X-ray data are shown in Fig. 9, together with the data by Hajdu *et al.*[16] As clearly seen in Fig. 9, the two intensity data show some appreciable discrepancies certainly. However, with respect to the intensity and position of the principal peak of $S_m(Q)_{calcd}$, the influence of the discrepancies on the final $S_m(Q)$ for neutrons through the calculated values of $S_c(Q)$ is within the range of experimental errors: concerning the peak intensities of $S_m(Q)$, it is within the range of circles and concerning the positional shift, within the range of vertical rod (Fig. 8). It is certain that this discrepancies does not affect the conclusion of the present study, and we have used the data by Narten and Levy on the whole.

The values of $x_5[1+S^{(00)}_{m,p}(Q)]$ calculated are shown together in Fig. 9. The overall agreement of the values with the experimental data is fairly good except in the range of $Q\lesssim 2$ Å^{-1}, though the factor $x_5[1+S^{(00)}_{m,p}(Q)]$ is the intra-pentamer contribution only. This shows that it is a main contribution to total intensities in the case of X-rays. And, to see in details, the calculated curves are in better agreement with the data of Narten at various temperatures on the whole, except for the deviation in the first peak[1] and that in the range of $Q=4.5$—6 Å^{-1}. Thus, the X-ray data also is expected to support the essential effectiveness of the pentamer-monomer mixture model as a whole.

Discussion and Conclusions

Physical Meaning of the Ingredient of $S_m(Q)$. In the preceding sections we have shown that the pentamer–monomer mixture model with a due assignment of x_5 value is a best structure model in the interpretation of neutron diffraction data at 25—95 °C. Here, overall features of the temperature variation of $S_m(Q)_{calcd}$ for the model are shown in Fig. 10. It is clear in the figure that the intensities in the hump at *ca.* 4 Å^{-1} as well as those in the main peak at 2 Å^{-1} decrease gradually with increasing temperature.

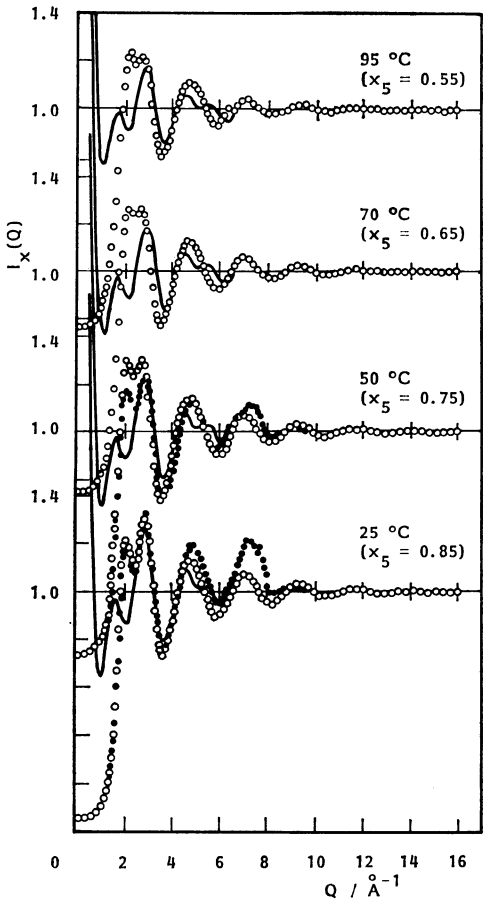

Fig. 9. The comparison between the calculated curves of $x_5[1+S^{(00)}_{m,p}(Q)]$ with the determined values of x_5 and the observed X-ray intensity data $I_x(Q)$.
○: Observed $I_x(Q)$ by Narten and Levy,[15] ●: observed $I_x(Q)$ by Hajdu *et al.*,[16] ——: $x_5[1+S^{(00)}_{m,p}(Q)]$.

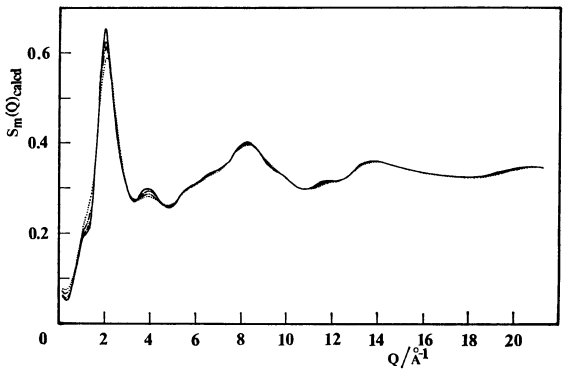

Fig. 10. Calculated $S_m(Q)$ for the pentamer–monomer mixture model.
——: $x_5=0.85$ (25 °C), - - -: $x_5=0.75$ (50 °C), —·—: $x_5=0.65$ (70 °C), ·····: $x_5=0.55$ (95 °C).

Table 1. The observed absolute neutron scattering factor $S_m(Q)$ as a function of scattering vector $Q/Å^{-1}$ for heavy water

$Q/Å^{-1}$	25 °C		50 °C		70 °C		95 °C	
	$2\theta=40°$	$2\theta=65°$	$2\theta=40°$	$2\theta=65°$	$2\theta=40°$	$2\theta=65°$	$2\theta=40°$	$2\theta=65°$
1.40	0.362		0.358		0.389		0.412	
1.45	0.361		0.374		0.386		0.411	
1.50	0.387		0.391		0.394		0.439	
1.55	0.407		0.413		0.407		0.448	
1.60	0.444		0.448		0.436		0.467	
1.65	0.479		0.485		0.472		0.490	
1.70	0.512		0.510		0.505		0.519	
1.75	0.548		0.542		0.533		0.542	
1.80	0.583		0.566		0.562		0.565	
1.85	0.607		0.590		0.592		0.582	
1.90	0.630		0.612		0.610		0.598	
1.95	0.642		0.629		0.629		0.614	
2.00	0.645		0.638		0.638		0.622	
2.05	0.638		0.637		0.636		0.627	
2.10	0.621		0.626		0.626		0.625	
2.15	0.597		0.608		0.608		0.613	
2.20	0.570		0.585		0.587		0.598	
2.25	0.544		0.557		0.565		0.576	
2.30	0.515		0.530		0.542		0.555	
2.35	0.490		0.507		0.519		0.533	
2.40	0.467		0.484		0.497		0.510	
2.45	0.446		0.462		0.475		0.488	
2.50	0.426	0.454	0.442	0.461	0.453	0.478	0.466	0.492
2.55	0.407	0.431	0.422	0.428	0.430	0.454	0.444	0.467
2.60	0.390	0.411	0.402	0.402	0.409	0.431	0.421	0.442
2.65	0.373	0.389	0.384	0.386	0.390	0.409	0.402	0.417
2.70	0.358	0.377	0.366	0.373	0.371	0.395	0.384	0.405
2.75	0.344	0.363	0.351	0.360	0.354	0.375	0.366	0.387
2.80	0.330	0.348	0.336	0.344	0.337	0.358	0.349	0.367
2.85	0.319	0.331	0.323	0.331	0.323	0.334	0.335	0.347
2.90	0.308	0.312	0.312	0.315	0.311	0.316	0.322	0.328
2.95	0.300	0.299	0.303	0.305	0.301	0.301	0.311	0.311
3.00	0.293	0.287	0.294	0.295	0.295	0.291	0.303	0.296
3.05	0.287	0.282	0.288	0.284	0.288	0.284	0.295	0.287
3.10	0.284	0.280	0.283	0.279	0.283	0.280	0.289	0.283
3.15	0.280	0.277	0.280	0.275	0.279	0.277	0.284	0.277
3.20	0.278	0.277	0.278	0.273	0.276	0.276	0.281	0.275
3.25	0.278	0.278	0.277	0.274	0.275	0.277	0.280	0.273
3.30	0.279	0.279	0.277	0.278	0.275	0.278	0.280	0.272
3.35	0.282	0.282	0.278	0.281	0.277	0.280	0.280	0.272
3.40	0.284	0.283	0.278	0.284	0.278	0.281	0.281	0.272
3.45	0.286	0.287	0.282	0.287	0.281	0.283	0.282	0.272
3.50	0.288	0.291	0.284	0.289	0.283	0.286	0.283	0.276
3.55	0.291	0.293	0.285	0.291	0.284	0.288	0.284	0.277
3.60	0.292	0.295	0.287	0.292	0.285	0.290	0.285	0.277
3.65	0.293	0.294	0.289	0.293	0.287	0.291	0.285	0.278
3.70	0.295	0.295	0.291	0.294	0.289	0.290	0.286	0.279
3.75	0.296	0.296	0.292	0.295	0.290	0.290	0.286	0.279
3.80	0.296	0.297	0.293	0.296	0.289	0.290	0.286	0.279
3.85	0.297	0.299	0.283	0.296	0.290	0.290	0.287	0.279
3.90	0.297	0.299	0.293	0.296	0.289	0.290	0.287	0.280
3.95	0.297	0.298	0.294	0.295	0.289	0.288	0.286	0.280
4.00	0.297	0.298	0.294	0.294	0.287	0.287	0.286	0.280
4.05	0.296	0.297	0.293	0.292	0.286	0.286	0.285	0.281
4.10	0.295	0.296	0.292	0.291	0.285	0.284	0.284	0.281
4.15	0.293	0.295	0.290	0.288	0.283	0.284	0.283	0.281
4.20	0.290	0.293	0.288	0.287	0.281	0.282	0.282	0.280
4.25	0.288	0.290	0.285	0.284	0.280	0.279	0.281	0.280
4.30	0.286	0.288	0.283	0.281	0.278	0.279	0.278	0.276
4.35	0.284	0.285	0.281	0.278	0.277	0.276	0.278	0.276
4.40	0.281	0.282	0.279	0.276	0.276	0.274	0.277	0.274
4.45	0.278	0.278	0.276	0.273	0.274	0.272	0.275	0.274
4.50	0.275	0.274	0.274	0.271	0.272	0.270	0.274	0.272
4.55	0.273	0.271	0.272	0.268	0.270	0.268	0.274	0.271
4.60	0.270	0.268	0.271	0.266	0.269	0.266	0.273	0.270
4.65	0.268	0.267	0.269	0.263	0.268	0.265	0.271	0.269
4.70	0.266	0.265	0.268	0.262	0.267	0.264	0.270	0.268
4.75	0.265	0.263	0.267	0.260	0.266	0.263	0.270	0.267
4.80	0.263	0.262	0.267	0.260	0.266	0.263	0.270	0.267
4.85	0.262	0.260	0.266	0.259	0.265	0.263	0.269	0.266
4.90	0.262	0.260	0.265	0.259	0.265	0.264	0.270	0.265
4.95	0.263	0.259	0.264	0.259	0.265	0.264	0.270	0.265
5.00	0.263	0.260	0.264	0.259	0.266	0.264	0.271	0.264
5.10	0.263	0.262	0.265	0.261	0.266	0.266	0.273	0.265
5.20	0.265	0.265	0.268	0.264	0.269	0.268	0.275	0.267
5.30	0.289	0.265	0.271	0.266	0.271	0.270	0.279	0.269
5.40	0.272	0.270	0.274	0.271	0.274	0.274	0.282	0.273
5.50	0.276	0.276	0.278	0.276	0.278	0.280	0.285	0.277
5.60	0.281	0.281	0.283	0.281	0.282	0.284	0.289	0.281
5.70	0.286	0.287	0.287	0.286	0.286	0.289	0.293	0.286
5.80	0.290	0.292	0.291	0.290	0.290	0.294	0.297	0.291
5.90	0.295	0.297	0.295	0.295	0.295	0.299	0.302	0.297
6.00	0.300	0.301	0.300	0.300	0.300	0.303	0.306	0.302
6.10	0.304	0.305	0.304	0.305	0.303	0.307	0.310	0.307
6.20	0.309	0.309	0.309	0.309	0.308	0.311	0.313	0.312
6.30	0.314	0.312	0.313	0.314	0.313	0.314	0.318	0.316
6.40	0.318	0.316	0.318	0.317	0.318	0.322	0.322	0.321
6.50	0.322	0.320	0.322	0.322	0.321	0.322	0.326	0.325
6.60	0.325	0.323	0.326	0.325	0.324	0.325	0.329	0.330
6.70	0.330	0.326	0.330	0.328	0.328	0.328	0.333	0.334
6.80	0.334	0.329	0.334	0.331	0.331	0.331	0.336	0.337
6.90	0.337	0.332	0.338	0.335	0.335	0.333	0.339	0.340
7.00	0.341	0.336	0.342	0.338	0.339	0.337	0.342	0.344
7.10	0.344	0.339	0.346	0.340	0.342	0.339	0.344	0.346
7.20	0.347	0.342	0.349	0.342	0.345	0.342	0.347	0.348
7.30	0.350	0.345	0.352	0.345	0.348	0.344	0.351	0.351
7.40	0.353	0.348	0.355	0.346	0.351	0.357	0.353	0.353
7.50	0.355	0.351	0.357	0.349	0.354	0.349	0.356	0.355
7.60	0.358	0.353	0.360	0.351	0.356	0.351	0.358	0.358
7.70	0.360	0.354	0.362	0.353	0.358	0.353	0.360	0.359
7.80	0.361	0.357	0.364	0.354	0.359	0.354	0.361	0.361
7.90	0.361	0.359	0.366	0.356	0.361	0.355	0.362	0.362
8.00	0.362	0.360	0.367	0.357	0.362	0.357	0.363	0.363
8.10	0.362	0.361	0.368	0.358	0.362	0.358	0.363	0.363
8.20	0.362	0.362	0.369	0.359	0.363	0.356	0.363	0.363
8.30	0.362	0.362	0.369	0.359	0.363	0.358	0.363	0.363
8.40	0.361	0.361	0.368	0.359	0.362	0.358	0.362	0.362
8.50	0.360	0.360	0.367	0.359	0.361	0.358	0.361	0.362
8.60	0.359	0.360	0.366	0.359	0.359	0.357	0.360	0.360
8.70	0.357	0.358	0.364	0.359	0.358	0.356	0.358	0.360
8.80	0.355	0.357	0.363	0.358	0.356	0.355	0.355	0.358
8.90	0.354	0.355	0.361	0.357	0.355	0.353	0.353	0.357
9.00	0.352	0.353	0.359	0.355	0.353	0.352	0.351	0.356
9.10	0.350	0.350	0.356	0.353	0.351	0.350	0.348	0.355
9.20	0.348	0.347	0.354	0.351	0.349	0.348	0.346	0.353
9.30	0.346	0.345	0.352	0.348	0.346	0.345	0.344	0.350
9.40	0.344	0.342	0.350	0.345	0.344	0.342	0.342	0.347
9.50	0.342	0.339	0.348	0.342	0.339	0.339	0.340	0.344
9.60	0.340	0.336	0.345	0.339	0.340	0.336	0.338	0.341
9.70	0.338	0.334	0.343	0.337	0.338	0.333	0.335	0.338
9.80	0.336	0.331	0.341	0.335	0.335	0.330	0.333	0.336
9.90	0.333	0.329	0.340	0.333	0.333	0.328	0.332	0.334
10.00	0.331	0.326	0.337	0.330	0.331	0.325	0.330	0.331
10.10	0.330	0.323	0.335	0.327	0.328	0.322	0.328	0.329
10.20	0.328	0.321	0.333	0.325	0.326	0.320	0.326	0.327
10.30	0.326	0.319	0.331	0.323	0.324	0.318	0.324	0.325
10.40	0.324	0.317	0.328	0.321	0.322	0.317	0.322	0.324
10.50	0.321	0.315	0.325	0.319	0.319	0.316	0.319	0.315

In order to elucidate further the physical meaning of temperature dependence of the structure factor $S_m(Q)$, we examine ingredients of the $S_m(Q)$, by considering the terms in Eq. 18. As clearly seen in Fig. 11, the first peak is mainly composed of the sum of the curve (a)$\equiv f_1(Q)$ and the curve (c)$\equiv \bar{f}_{2U}(Q)[S_c(Q)-1]$, expressing the averaged separation between two adjacent centers of water molecules to be about 3 Å, and, on the other hand, the hump at *ca.* 4 $Å^{-1}$ is originated from the curve (b)$\equiv (x_5/5)f_c^5(Q)$, which is ascribed to the presence of the tetrahedral pentamer. The sum of curves (a) and (c) ($\equiv f_1(Q)+\bar{f}_{2U}(Q)[S_c(Q)-1]$) corresponds to the $S_m(Q)$ for completely-uncorrelated (at molecular level) orientation model, as described by Egelstaff, Page and Powles.[12,13] Hence, it is stated that the contribution of curve (b) (Eq. 20) originated from the presence of the tetrahedral pentamers forms the essential character of the liquid structure of water, producing the hump at *ca.* 4 $Å^{-1}$ in the $S_m(Q)$ curves.

Concluding Remarks. Neutron structure factors $S_m(Q)$ of D_2O were determined at 25, 50, 70, and 95 °C. The diffraction data were analyzed by using a general expression of $S_m(Q)$ derived from a new

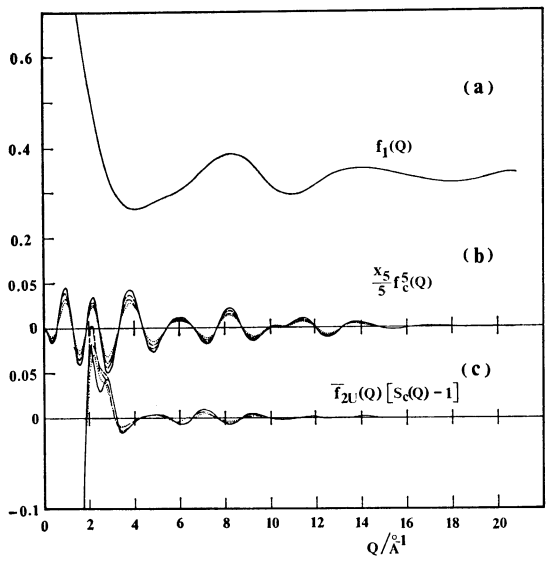

Fig. 11. Contributions of (a) $f_1(Q)$ (Eq. 19), (b) $\frac{x_5}{5}f_c^5(Q)$ (Eq. 20), and (c) $\bar{f}_{2U}(Q)[S_c(Q)-1]$ to the $S_m(Q)_{calcd}$ (Eq. 18).
——: $x_5=0.85$, - - -: $x_5=0.75$, —·—: $x_5=0.65$, ……: $x_5=0.55$.

theoretical procedure of analysis which is generally applicable to the fluid system composed of molecular clusters with various sizes. The following conclusions were obtained:

1) The pentamer–monomer mixture model with the due value of pentamer fraction x_5 assigned is the best one as a fundamental structure model of water at temperatures, 25—95 °C, for the explanation of diffraction data.

2) The x_5 values determined by fitting the $S_m(Q)_{calcd}$ with the $S_m(Q)_{obsd}$ at each temperature are $x_5=0.85\pm0.05$ at 25 °C, $x_5=0.75\pm0.05$ at 50 °C, $x_5=0.65\pm0.05$ at 70 °C, and $x_5=0.55\pm0.05$ at 95 °C, respectively.

3) The decrease of x_5 with temperature rise indicates the destruction of pentamers expected at elevated temperatures and the effect of the destruction appears mainly as the gradual decrease of intensities in the first peak at 2 Å^{-1} and the hump at *ca.* 4 Å^{-1} in the neutron structure factor curves.

4) The hump at *ca.* 4 Å^{-1} in the $S_m(Q)$ curves is originated from the presence of the tetrahedral pentamers forming the essential character of the liquid structure of water.

References

1) N. Ohtomo, K. Tokiwano, and K. Arakawa, *Bull. Chem. Soc. Jpn.*, **54**, 1802 (1981).
2) N. Ohtomo and K. Arakawa, *Bull. Chem. Soc. Jpn.*, **51**, 1649 (1978).
3) N. Ohtomo and K. Arakawa, *Bull. Chem. Soc. Jpn.*, **53**, 1510 (1980).
4) N. Ohtomo, K. Arakawa, M. Takeuchi, T. Yamaguchi, and H. Ohtaki, *Bull. Chem. Soc. Jpn.*, **54**, 1314 (1981).
5) J. G. Powles, *Mol. Phys.*, **26**, 1325 (1973): **36**, 1181 (1978).
6) J. G. Powles, *Mol. Phys.*, **42**, 757 (1981).
7) J. P. Hansen and I. R. McDonald, "Theory of Simple Liquids," Academic Press, London (1976), Chap. 5.
8) K. E. Gubbins, C. G. Gray, P. A. Egelstaff, and M. S. Ananth, *Mol. Phys.*, **25**, 1353 (1973).
9) J. J. Weis and D. Levesque, *Phys. Rev. A*, **13**, 450 (1976).
10) K. Arakawa, K. Tokiwano, and K. Kojima, *Bull. Chem. Soc. Jpn.*, **50**, 65 (1977).
11) K. Arakawa, "Water and Metal Cations in Biological System," ed by B. Pullman and K. Yagi, Japan Scientific Societies Press, Tokyo (1980), pp. 13—29.
12) P. A. Egelstaff, D. I. Page, and J. G. Powles, *Mol. Phys.*, **20**, 881 (1971).
13) D. I. Page and J. G. Powles, *Mol. Phys.*, **21**, 901 (1971).
14) With respect to the assignment of Debye-Waller factors, the magnitude of mean-square variation $2\gamma_{nn'}$ is estimated to be 0.06 Å per 1 Å of interatomic distance $r_{nn'}$, assuming $\gamma_{nn'} \propto r_{nn'}$, throughout all the present calculations.[2)]
15) A. H. Narten and H. A. Levy, *J. Chem. Phys.*, **55**, 2263 (1971).
16) F. Hajdu, S. Lengyel, and G. Pálinkás, *J. Appl. Cryst.*, **9**, 134 (1976).
17) G. Walford and J. C. Dore, *Mol. Phys.*, **34**, 21 (1977): In this work, they have reported neutron diffraction data for heavy water at temperatures, 11—79 °C, in which the same trend as seen in our present data has been observed. However, their data are unreliable for its experimental inaccuracy because "it was discovered that the incident beam was contaminated by a contribution from 2.26 Å neutrons (arising from second-order reflections in the monochrometor) which was estimated to be 28 per cent" as they stated in their article.